

Original articles

Research article

<https://doi.org/10.17308/kcmf.2025.27/13300>

Hydration properties of heterogeneous ion exchange membranes after their long-term use in the electrodialysis treatment of wastewater from the production of mineral fertilizers

O. A. Kozaderova[✉], I. A. Saranov

Voronezh State University of Engineering Technologies
Revolution ave., 19, Voronezh 394036, Russian Federation

Abstract

Objectives: In this paper, the evolution of the hydration characteristics of heterogeneous cation- and anion-exchange membranes during the electrodialysis treatment of multicomponent salt solutions is studied.

Experimental: The objects of research are heterogeneous RalexCMH-Pes (sulfocation exchange) and RalexAMH-Pes (anion exchange with quaternary ammonium groups) membranes, which have been used with different durations in an industrial electrodialyzer for the concentration/desalination of liquid waste from the production of complex mineral fertilizers. The hydration characteristics of the membranes were determined using synchronous thermal analysis. The morphology of the surface of the studied membranes was investigated by scanning electron microscopy. X-ray phase analysis of the ash residue after annealing of the membranes was carried out using the diffractometric method.

Conclusions: The moisture content and specific heat of dehydration of the studied membranes increase during long-term electrodialysis processing of liquid waste from the production of complex mineral fertilizers. For cation-exchange and anion-exchange membranes, the moisture content increases by 74 and 68 %, respectively. The predominant type of kinetically unequal water in membranes is weakly and moderately bound water. Strongly bound water molecules involved in ion-dipole interactions with active functional groups are least represented in membranes, and during operation in an electrodialyzer, their proportion increases by 1.35 times in the case of cation-exchange membranes and decreases by 1.3 times in anion-exchange membranes. The increase in moisture content and the redistribution of water fractions of different degrees of binding can be explained by the degradation of membranes caused by their morphological changes (an increase in the number of defects and the size of macropores filled with solution or water), as well as the stretching of the membrane matrix due to the presence of large and highly hydrated ions in the processed liquid waste. In addition, hydrophilic inorganic precipitates accumulate in the nanopores of anion-exchange membranes.

Keywords: Heterogeneous ion exchange membranes, Degradation, Electrodialysis, Hydration characteristics, Synchronous thermal analysis

Funding: The study was supported by the Russian Science Foundation (RSF), project No. 25-29-00557, <https://rscf.ru/en/project/25-29-00557/>

Acknowledgements: Synchronous thermal analysis was performed on the equipment of the Test Center of the Voronezh State University of Engineering Technologies. The studies using scanning electron microscopy and X-ray diffractometry were performed on the equipment of the Center for Collective Use of Scientific Equipment of the Voronezh State University

For citation: Kozaderova O. A., Saranov I. A. Hydration properties of heterogeneous ion exchange membranes after their long-term use in the electrodialysis treatment of wastewater from the production of mineral fertilizers. *Condensed Matter and Interphases*. 2025;27(4): 615–629. <https://doi.org/10.17308/kcmf.2025.27/13300>

Для цитирования: Козадерова О. А., Саранов И. А. Гидратационные свойства гетерогенных ионообменных мембран после их длительного использования в электродиализной переработке сточных вод производства минеральных удобрений. *Конденсированные среды и межфазные границы*. 2025;27(4): 615–629. <https://doi.org/10.17308/kcmf.2025.27/13300>

[✉] Olga A. Kozaderova, e-mail: kozaderova-olga@mail.ru

© Kozaderova O. A., Saranov I. A., 2025



The content is available under Creative Commons Attribution 4.0 License.

1. Introduction

The first commercial electrodialyzer was manufactured in the 1950s and was used to desalinate brackish water [1]. Currently, electrodialysis (ED) is widely used in the chemical [2], pharmaceutical [3], and food [4] industries. At the same time, special attention should be paid to the use of this electromembrane method for the extraction of useful components from industrial and municipal wastewater [5–7] and the creation of waste-free production of organic products [8–11]. In particular, the use of electrodialysis technology for the treatment of wastewater from the production of mineral fertilizers [12–14], which are multicomponent solutions and/or mixtures of inorganic and organic compounds, is quite promising.

During the electrodialysis processing of such media containing a wide range of different components, under conditions of direct current, elevated temperature and pH changes, the degradation of ion exchange membranes (IEM) used in electrodialyzers occurs [15]. Due to the presence of polluting components in the treated media and/or due to the initiation of undesirable processes in the membranes, such as precipitation accumulation, changes in morphology, and linear pore sizes, the physico-chemical, electrochemical, and transport characteristics of IEM deteriorate and the efficiency of the electrodialysis process as a whole decreases [16]. The problem of IEM degradation is encountered during the electrodialysis treatment of municipal wastewater [12,17], natural waters [18,19], food industry solutions [20–22], and pharmaceutical industry [23], as well as of IEM artificially aged in the laboratory [24,25]. At the same time, ED technology is being actively implemented in a number of enterprises for the production of mineral fertilizers, including JSC "Minudobreniya" and JSC "Kuibyshevazot", as part of projects for processing steam condensate [26]. It is planned to put ED equipment into operation at JSC NAK Azot, JSC TAIF-NK, and JSC Achinsk Oil Refinery [26]. However, despite the active introduction of this technology, there are few studies on the degradation of IEM during the electrodialysis of waste from the production of mineral fertilizers [10, 27]. This makes it difficult to predict the

duration of effective and useful use of IEM in ED installations, which significantly depend on the degree of membrane degradation. This negative process is accompanied by changes in the structure and chemical composition of the membranes [15, 16, 28], which largely determine their selectivity and transport characteristics.

In turn, the structure, transport, and physico-chemical properties of ion-exchange membranes depend significantly on their interaction with water. Membranes function effectively only in the hydrated state, when they are capable of separation and ion exchange due to a significant weakening of the electrostatic interaction between counterions and fixed ions [29]. Deterioration of the transport properties of membranes in conditions of low humidity is one of the main problems limiting the practical application of ion exchange membranes. It was shown in [30] that an increase in moisture content is possible due to modification of the membrane by doping with inorganic nanoparticles, which, at low humidity, participate in ion transport, and the water molecules sorbed by them participate in the hydration of alkali metal cations in the membranes.

High moisture content is one of the main conditions for the formation of an optimal hydrophilic/hydrophobic balance of the ion surface, which, in turn, significantly affects the efficiency parameters of the separation process during electrodialysis, including the intensity of electroconvection and the generation of H^+ and OH^- ions occurring at the membrane/solution interface [31]. For example, it was shown in [32] that hydrophobic amino acids adsorbed on the membrane surface contribute to an increase in its hydrophobicity, which leads to a greater contribution of electroconvection to mass transfer during intensive current modes of electrodialysis.

Heterogeneous IEM are characterized by a higher moisture content, lower temperatures of the onset of dehydration, and a higher relative rate of water release compared to ion-exchange resins, on the basis of which they are manufactured [33]. The features of the interaction of such IEM with a solvent are largely determined by pores of different sizes. Porometric analysis of domestic heterogeneous MK-40 and MA-41

membranes showed [34, 35] that the thinnest pores (mainly with a radius of 3.5 and 13 nm) are located in ion exchanger grains, whereas pores with a radius of 100 nm are formed at the contact points of ion exchange resin and polyethylene particles, and the largest pores with an effective radius of 3 microns are formed between the reinforcing fabric and the ion exchanger/polyethylene composite. Depending on the different levels of membrane structural organization (molecular, supramolecular, macroscopic), several structural, kinetically unequal types of water in the membranes are distinguished: "bound", "intermediate", and "free" [36]. When the nature of the counterion changes, the water content and state inside the ion exchange membrane change [36]. Thus, an urgent task is to determine the hydration characteristics of ion exchangers depending on the type of membrane and the duration of use in electrodialysis plants.

To solve this problem, thermal analysis methods are used: thermogravimetry (TG) and differential thermal analysis (DTA), based on recording the parameters of the system under study, which change under conditions of programmed temperature exposure [33]. The thermogravimetry method consists in measuring the mass loss of the test material as the temperature changes. With the help of differential thermal analysis, the thermal effects of transformations occurring in the test sample under temperature influence are recorded. Synchronization of TG and DTA measurements makes it possible not only to determine the range of thermal stability of the ion exchange materials under study, but also to obtain information about the physico-chemical properties of the water contained in them, as well as to establish the main characteristics of the dehydration process of ion exchangers [33]. The experimental results obtained in this work using several complementary methods (thermal analysis, scanning electron microscopy, and X-ray diffraction) make it possible to reasonably establish the role of morphological changes and precipitation accumulation as the most likely causes of the evolution of hydration characteristics of heterogeneous ion-exchange membranes observed during electrodialysis

treatment of multicomponent salt solutions (waste products of complex mineral fertilizers), which is the **purpose** of this study.

2. Experimental

2.1. Membranes

The research objects were RalexCMH-Pes (sulfocation exchange) and RalexAMH-Pes (anion exchange with quaternary ammonium groups) membranes manufactured by Mega JSC (Czech Republic) [37]. They are heterogeneous and contain an ion exchanger, plasticizer (polyethylene), and reinforcing fabric (polyester).

The membranes were operated in an industrial electrodialyzer with alternating cation- and anion-exchange membranes separated by flow turbulator grids in the mode of concentration/desalination of multicomponent salt solutions, such as waste from the production of complex mineral fertilizers for different periods of time. The membranes separated the concentrate/dilute chambers and did not come into contact with the solutions of the electrode chambers. The process was carried out in pre-limit current modes. The composition of treated wastewater is as follows (mg/dm³): Ca²⁺ 0.9–6.7; Cl⁻ 1.3–16.9; Mg²⁺ 0.2–3.8; SO₄²⁻ 2.2–39.8; Na⁺ 0.10; F⁻ 3.2–92.3; K⁺ 0.15; NO₃⁻ 15.4–312.1; Fe²⁽³⁾⁺ 0.01–0.17; PO₄³⁻ 0.6–2.3; NH₄⁺ 15.9–258.5 [27, 38]. After removing the membranes from the electrodialyzer, they were washed in distilled water, the surface was cleaned with a soft sponge and placed in distilled water. The characteristics of the used membranes were compared with similar characteristics of the initial samples that were not involved in the electrodialysis process.

The conditioning of the initial membranes was carried out in accordance with the methods given in [39]. First, salt treatment was performed in NaCl solutions of different concentrations, then the cation exchange membranes were treated with acid, and the anion exchange membranes with alkali. After conditioning, the cation exchange samples were converted to the Na⁺ form, and the anion exchange samples were converted to the Cl⁻ form and stored in distilled water.

In this paper, the pristine conditioned samples have the index "prist", the membranes for one

year of use are “1”, five years are “2”. CEM and AEM are the designations of cation- and anion-exchange membranes, respectively. The main characteristics of the studied membranes are given in Table 1.

2.2. Methods

The morphology of the surface of the studied IEM was studied using scanning electron microscopy (SEM) on a JSM-6380 LV device (Japan). The preparation of the membranes for analysis was as follows. The membranes (AEM_{prist}, AEM₁, AEM₂, CEM_{prist}, CEM₁, CEM₂) stored in distilled water were dried in a drying cabinet to a constant weight at 70 °C, 5×5 mm samples were cut out, and an electrically conductive carbon layer was sprayed on them.

X-ray phase analysis of the ash residue after IEM annealing at 600 °C was performed using an ARL X'TRA diffractometer (Thermo Scientific, Switzerland). The particle size of the mineral components present in the membrane was calculated from the width of the diffraction maximum using the Scherrer formula [40].

Experimental studies of the membrane dehydration process were carried out using a NETZSCH STA 449 F3 Jupiter synchronous thermal analysis device combining high-precision thermal weights and a differential scanning calorimeter. The device allows one to simultaneously obtain a set of several interrelated thermoanalytical curves: two integral curves (the mass loss curve (TG) and the thermal effects curve (DSC)), as well as their corresponding two differential curves (the mass loss rate curve (DTG) and the curve of the rate of change of the thermal effect (dDSC)). Swollen samples of IEM, previously soaked in distilled water for at least 7 days, were studied. Temperature research program: heating from 298 to 523 K at a rate of 5 K/min. Research conditions: aluminum crucibles, nitrogen atmosphere, purge gas consumption at 15 cm³/min. The received thermograms were

processed using NETZSCH Proteus and MS Excel software.

3. Results and discussion

Typical experimental thermoanalytical curves are shown in Fig. 1 using a CEM_{prist} membrane sample as an example. Similar thermograms in the form of a set of TG, DTG, DSC, and dDSC curves were obtained for the five other membranes studied in the work (AEM_{prist}, AEM₁, AEM₂, CEM₁, CEM₂). The experimental thermoanalytical curves were rearranged and shown in Fig. 2 and 3 in a modified temperature-time format used in works on the thermal analysis of ion-exchange materials [33, 41]. This format for representing thermal curves allows not only to identify, but also to visually compare the integral TG, DSC, and differential DTG effects observed when samples are heated, which makes it possible, among other things, to detect the difference between the original and spent membranes.

It is important to note that for all studied IEM samples, regardless of the type of membranes (cation or anion exchange) and the duration of their use in an electrodialysis unit, the change in mass Δm , determined by the integral thermogravimetric TG curve, is consistent with the deviation of the differential thermal DSC curve from the baseline in the temperature range of 300–430 K. In addition, the highest rate of mass loss of the membrane sample, determined by the minimum on the DTG curve, is observed at a temperature close to the temperature of the DSC maximum (for example, at $T_{\max}^{\Delta m} = 67.5$ °C for the CEM_{prist} membrane sample). This agreement of the TG, DTG, and DSC curves can be explained by the fact that the changes observed on them are due to a single process, the removal of water (dehydration) from the membrane sample when it is heated. Indeed, according to [33], the decrease in the mass of ion-exchange material in the temperature range of 300–430 K, in which the most significant change in Δm for the studied membranes is observed on

Table 1. Characteristics of ion exchange membranes

Parameter	CEM _{prist}	CEM ₁	CEM ₂	AEM _{prist}	AEM ₁	AEM ₂
Exchange capacity, mmol/g of dry membrane	1.6±0.1	1.7±0.1	1.6±0.1	1.5±0.1	1.5±0.1	1.2±0.1
Thickness, mm	508±2	511±1	513±2	507±1	510±1	512±2

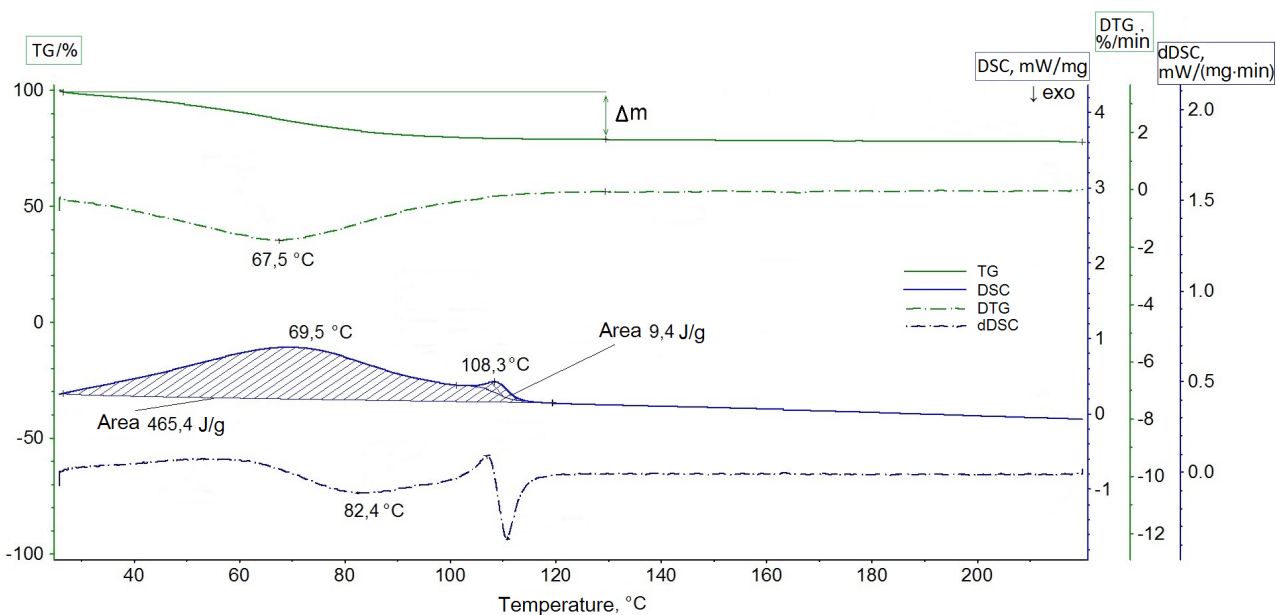


Fig. 1. Experimental thermoanalytical curves obtained for the CEM_{prist} membrane sample. Notation: TG is the mass loss curve, DSC is the thermal effects curve, DTG is the curve of the mass loss rate, dDSC is the curve of the rate of the thermal effect change

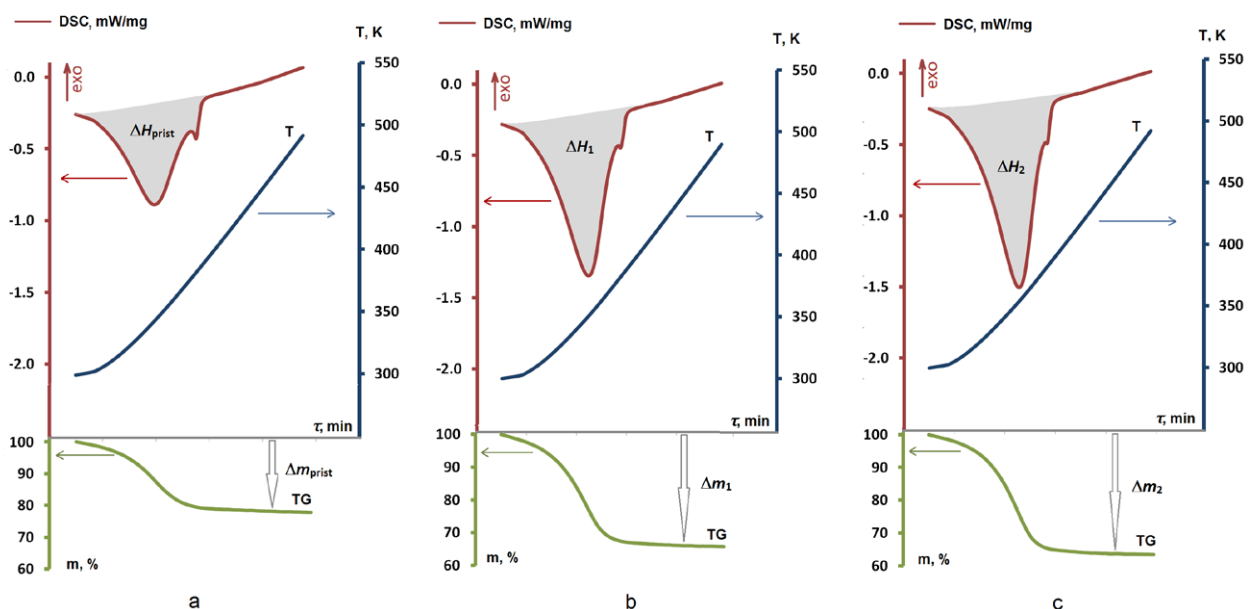


Fig. 2. Thermal curves of cation exchange membranes: CEM_{prist} (a), CEM₁ (b), CEM₂ (c). Notation: T is the temperature change curve, TG is mass loss curve, DSC is the thermal effects curve; Δm_{prist} , Δm_1 , Δm_2 – mass change, ΔH_{prist} , ΔH_1 , ΔH_2 – specific heat of dehydration (J/g) for samples CEM_{prist} (a), CEM₁ (b), CEM₂ (c) respectively

all the obtained thermoanalytical curves, is due precisely to the removal of water from them. Thus, a comparative assessment of the moisture content of the studied membranes can be carried out by the value of Δm . The specific moisture capacity

n_W (mol H₂O/mol functional group) was calculated using the formula:

$$n_W = \frac{\Delta m}{M_{H_2O} \cdot EC} \cdot 100 \%$$

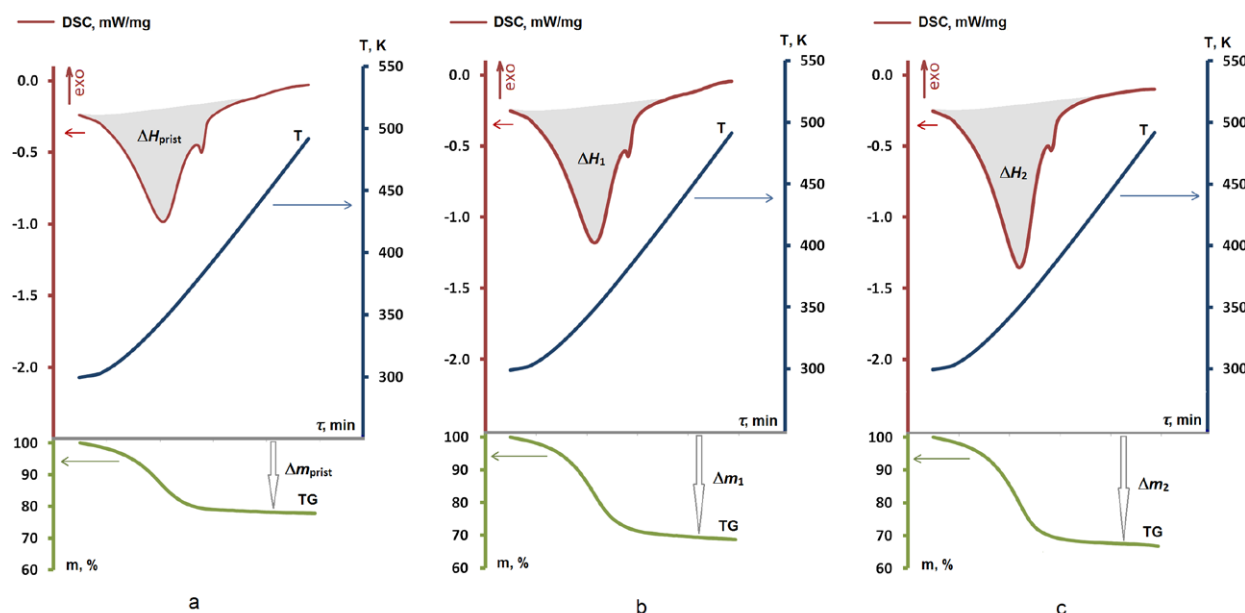


Fig. 3. Thermal curves of anion exchange membranes: AEM_{prist} (a), AEM₁ (b), AEM₂ (c). Notation: T is the temperature change curve, TG is mass loss curve, DSC is the thermal effects curve; Δm , Δm_{prist} , Δm_1 , Δm_2 – mass change, ΔH_{prist} , ΔH_1 , ΔH_2 – specific heat of dehydration (J/g) for samples AEM_{prist} (a), AEM₁ (b), AEM₂ (c) respectively

Here $M_{\text{H}_2\text{O}}$ is a molar mass of water, EC is an exchange capacity of the membrane (Table 1). In turn, the specific thermal effect of the endothermic dehydration process ΔH (the so-called “endoeffect” [33]) is determined by the area of the maximum observed on the DSC dependence. Using the example of a CEM_{prist} membrane sample, it can be seen (Fig. 1) that such a maximum with a peak at $T_{\text{max}} = 69.5$ °C is quite extensive, and its area, equal to $\Delta H = 465.4$ J/g, corresponds to the thermal effect of dehydration of this IEM, normalized by the mass of the initial membrane sample, i.e. represents the heat of dehydration. A small maximum at 108.3 °C can be attributed to the melting of an inert binder of heterogeneous IEM, polyethylene [43].

On the modified temperature-time dependences (Figs. 2 and 3), the minimum area on the DSC curve corresponds to the thermal effect. The complete set of quantitative characteristics of the dehydration process (Δm , $T_{\text{max}}^{\Delta m}$, T_{max} , ΔH), found from modified thermoanalytical curves, is given in Table 2 for all studied CEM and AEM samples. It follows from these data that the mass loss Δm increases with increasing duration of use of CEM and AEM membranes. This indicates

an increase in the moisture content of both cation and anion exchange membranes during operation of the electrodialysis unit. The specific heat of dehydration increases naturally, which is consistent with an increase in the moisture content of the membrane. It should be emphasized that the heat of dehydration, calculated per mole of removed water, practically does not depend on the type of membrane and the duration of its use, and averages 39.0 ± 1.8 and 35.8 ± 1.2 kJ/mol for CEM and AEM, respectively. According to [33], the values of the molar heat of dehydration in the range of 35–39 kJ/mol correspond to the formation of associates of 2–4 water molecules.

It is important to note the increase in temperature $T_{\text{max}}^{\Delta m}$, which corresponds to the highest rate of mass loss of the membrane sample: from 341 to 351 K in the range CEM_{prist} < CEM₁ < CEM₂, and from 343 to 348 K in the range AEM_{prist} < AEM₁ < AEM₂. A similar effect of $T_{\text{max}}^{\Delta m}$ growth found for the MF-4-SK membrane in [42] is explained by the effect of an inorganic dopant (polysulfuric acid particles) on the system of pores and channels, the introduction of which into the volume of MF-4-SK leads to an increase in moisture content. Thus, an increase in the

Table 2. Quantitative characteristics of the membrane dehydration process

Ion exchange membrane	Δm , %	$T_{\max}^{\Delta m}$, K	T_{\max} , K	ΔH , J/g	ΔH , kJ/mol
CEM _{prist}	20.73	67.5	69.5	465.4	40.5
CEM ₁	33.43	74.9	77.5	693.8	37.3
CEM ₂	35.51	78.0	80.4	774.9	39.3
AEM _{prist}	24.73	70.2	72.8	476.8	34.7
AEM ₁	29.73	73.2	75.7	592.6	35.9
AEM ₂	32.08	75.4	77.5	654.5	36.8

temperature of the maximum water removal rate correlates with data on an increase in the parameters Δm and ΔH .

According to [33], the analysis of thermoanalytical curves, along with the determination of the membrane moisture content, makes it possible to quantify the total and relative content of kinetically unequal (weakly, moderately, and strongly bound) water molecules in the membranes. This assessment is based on the representation of the dehydration process of ion-exchange membranes as a sequential release of kinetically unequal water molecules characterized by different degree of binding [33]. In accordance with the procedure for processing TG dependencies described in [33], the thermoanalytical curves of the studied cation and anion exchange membranes are presented in the $\lg \alpha - T^{-1}$ coordinates, where $\alpha = \Delta m_i(T_i)/\Delta m$ is the ratio of the mass change of the membrane sample $\Delta m_i(T_i)$, corresponding to the amount released water at a temperature of T_i , to a total loss of mass. The slope of the $\lg \alpha - T^{-1}$ curve depends on the nature and energy of the interaction of water molecules in the membrane. As a result, the corresponding dependencies are characterized by the presence of three linear sections with different slopes, each of which corresponds to a specific stage of water removal. The removal of weakly bound water (dehydration stage I) is carried out by a low-temperature section based on the logarithmic dependence of the relative mass change of the membrane sample on T^{-1} . In this case, we are talking about H_2O molecules bound to each other by the weakest hydrogen bonds characteristic of the bulk phase of the solvent in the region of “long-range hydration” [33]. The intermediate medium-temperature section of the $\lg \alpha - T^{-1}$ curve corresponds to the

stage of dehydration II, the removal of water, in which intermolecular interactions, compared with weakly bound water, are enhanced due to the influence of membrane functional groups [33], as a result of which the slope of the $\lg \alpha$ dependence on T^{-1} decreases. Finally, the high-temperature section of the dependence of the relative change in the mass of the IEM sample on temperature, characterized by the lowest slope, corresponds to stage III of dehydration, that is the removal of water molecules involved in the strongest ion-dipole interactions with the functional groups of the membrane, Fig. 4.

The quantitative characteristics of water molecules of various degrees of binding, found by the dependence of $\lg \alpha$ on T^{-1} of the studied CEM and AEM membranes, are shown in Tables 3 and 4. A comparison of these data shows that all the studied ion exchange membranes are characterized by the highest content of weakly and also moderately bound water, while strongly bound water is represented to the least extent. The values of moisture capacity found are consistent with the data obtained in [33, 44–46]. In this case, the analysis of the relative distribution of the water content of various degrees of binding revealed differences for cation- and anion-exchange membranes in the change of their moisture content during long-term operation in an electrodialysis unit.

Thus, during the transition from CEM_{prist} to CEM₁ and CEM₂, cation exchange membranes are characterized by an increase in the fraction of strongly bound water molecules. Indeed, if this parameter is 9.6 % for the initial sample of a cation exchange membrane, then after one year and five years of use it increases to 12 and 13 %, respectively (Table 3). In the case of anion exchange membranes, the transition from

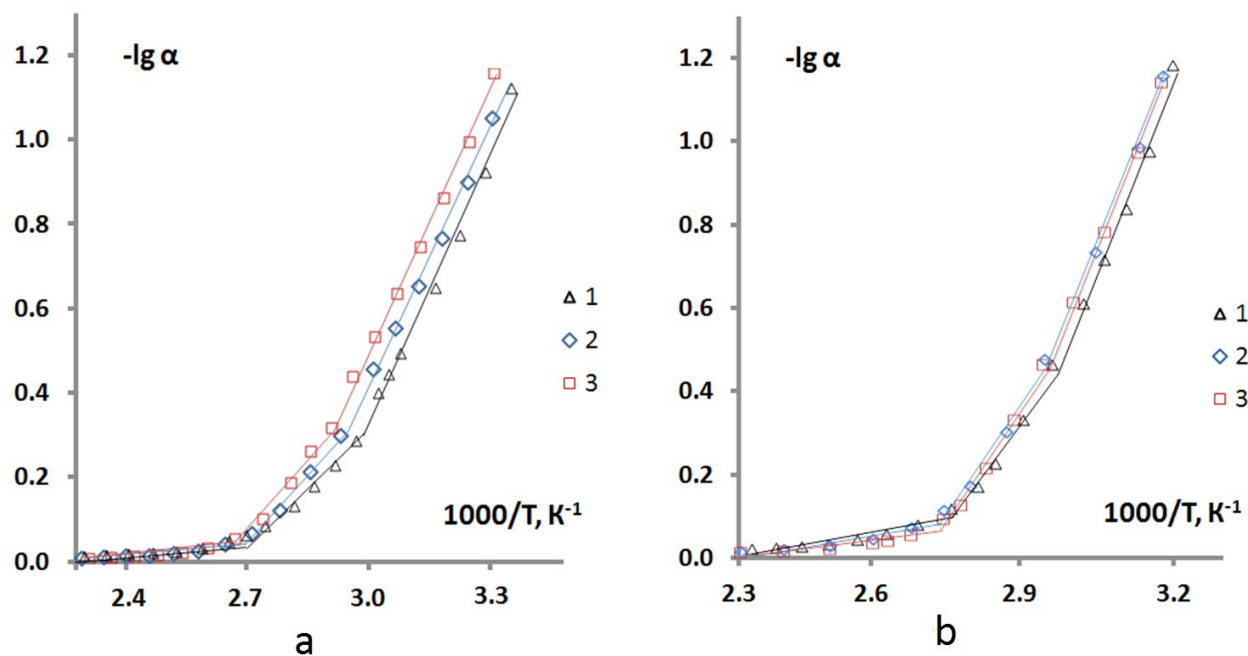


Fig. 4. Dependences of the relative change (α) in the mass of the membrane sample on temperature for cation exchange CEM (a) and anion exchange AEM (b) membranes: 1 - $\text{CEM}_{\text{prist}}$, $\text{AEM}_{\text{prist}}$; 2 - CEM_1 , AEM_1 ; 3 - CEM_2 , AEM_2

Table 3. Quantitative characteristics of kinetically unequal water in cation exchange membranes at maximal swelling

Membrane	Stage of dehydration	$\Delta T, \text{K}$	% H_2O	Specific moisture capacity $n_w, \text{mol H}_2\text{O/mol functional groups}$	
$\text{CEM}_{\text{prist}}$	I	298–331	39.7	3.7	$\Sigma = 9.3$
	II	331–369	50.5	4.7	
	III	369–402	9.6	0.9	
CEM_1	I	298–337	43.0	6.8	$\Sigma = 15.8$
	II	337–365	44.9	7.1	
	III	365–401	12.0	1.9	
CEM_2	I	298–340	40.1	6.5	$\Sigma = 16.2$
	II	340–365	46.9	7.6	
	III	365–410	13.0	2.1	

Table 4. Quantitative characteristics of kinetically unequal water in anion exchange membranes at maximal swelling

Membrane	Stage of dehydration	$\Delta T, \text{K}$	% H_2O	Specific moisture capacity $n_w, \text{mol H}_2\text{O/mol functional groups}$	
$\text{AEM}_{\text{prist}}$	I	298–329	33.3	3.8	$\Sigma = 11.4$
	II	329–359	47.4	5.4	
	III	359–419	19.3	2.2	
AEM_1	I	298–336	40.1	5.6	$\Sigma = 14.0$
	II	336–359	39.2	5.5	
	III	359–432	20.7	2.9	
AEM_2	I	298–337	40.4	7.8	$\Sigma = 19.3$
	II	337–362	44.6	8.6	
	III	362–429	15.0	2.9	

AEM_{prist} to AEM₂ is accompanied, on the contrary, by a decrease in the fraction of strongly bound water molecules from 19.3 to 15.0 % (Table 4). Accordingly, the fraction of weakly bound water in the internal solution of the anion exchange membrane increases from 33.3 to 40.4 %, which is consistent with the results of the analysis of the transport and structural characteristics of the studied IEM, for which, according to electrical conductivity data, an increase in the contribution of the internal solution to conductivity was found [47].

The discovered effects of increasing the moisture content of cation- and anion-exchange membranes during their long-term operation during electrodialysis of multicomponent solutions of mineral salts, as well as the revealed redistribution of water fractions of different degree of connectivity, may be due to a number of reasons.

One of the possible factors causing a change in both the moisture content and the redistribution of water of different degree of binding is the accumulation of precipitation in the pores of the membrane. It is known [30] that the introduction of inorganic dopants into the membrane matrix leads to an increase in the moisture content of the ion-exchange material. In this case, the immobilized nanoparticles replace part of the electroneutral solution in the inter-gel spaces of the membrane, which leads to an increase in their volume fraction and a simultaneous decrease in the fraction of the electroneutral solution in the membrane [48]. For cation exchange membranes, diffractometric analysis of calcination residues failed to detect significant differences between new (CEM_{prist}) and spent (CEM₁, CEM₂) samples. Consequently, sedimentation in cation exchange membranes during their long-term operation in an electrodialysis unit most likely does not occur. A similar effect of an increase in moisture content unrelated to precipitation was observed in [24] during prolonged exposure to temperature and pH variation of the solution.

A feature of the studied anion exchange membranes, on the contrary, is the formation of precipitation during operation in an ED installation. Despite the fact that mineral deposits formed during the use of AEM during the concentration/desalination of wastewater from

the production of complex mineral fertilizers are not visually detected during SEM analysis (Fig. 5), diffractometric analysis of the calcined residue of anion exchange membranes after one and five years of use showed the presence of the following substances in IEM: CaSO₄, Ca(H₂PO₄)₂, Fe₂O₃, Na₃PO₄ (AEM₁); Ca(OH)₂, Fe₂O₃, and Na₃PO₄ (AEM₂). The ash residue weights were 0.4 and 0.8 mg/g for AEM₁ and AEM₂, respectively, which indicates an increase in the proportion of mineral deposits in the volume of IEM during the operation of the membranes. The calculation of the particle size of the mineral components in the ash residue according to diffractometry data [40] showed that they have a diameter from 9 to 45 nm. This allows us to make an assumption about the localization of precipitation in IEM nanopores, which is consistent with the results of [40, 49]. The calculation of the relative moisture capacity leads to higher values for AEM₂ compared to CEM₂, which also correlates with the accumulation of precipitation in anion-exchange membranes and is consistent with data on an increase in moisture content in membranes doped with hydrated metal oxides [30]. In contrast to [48], in the present work, the appearance of sediment nanoparticles in the pores of the anion exchange membrane leads to a decrease in the proportion of strongly bound rather than weakly bound water. Considering that the moisture content of membranes is determined by complex internal interactions between water molecules, functional groups, and the hydrophobic matrix, it is difficult to expect an unambiguous dependence of this value on only one factor (precipitation) while changing others at the same time. Moreover, in the case of both types of membranes, the main factor in the increase in moisture content appears to be an increase in the number and size of pores and/or defects in the heterogeneous sample due to membrane degradation during prolonged operation in an electrodialysis unit.

To confirm this assumption, we analyzed the SEM images of the surface of the studied membranes shown in Figs. 5 and 6. The main surface material of the IEM is a composite: polyethylene with ion exchange resin particles fairly evenly distributed in it. In addition, cavities (voids) are visible on the surface for all

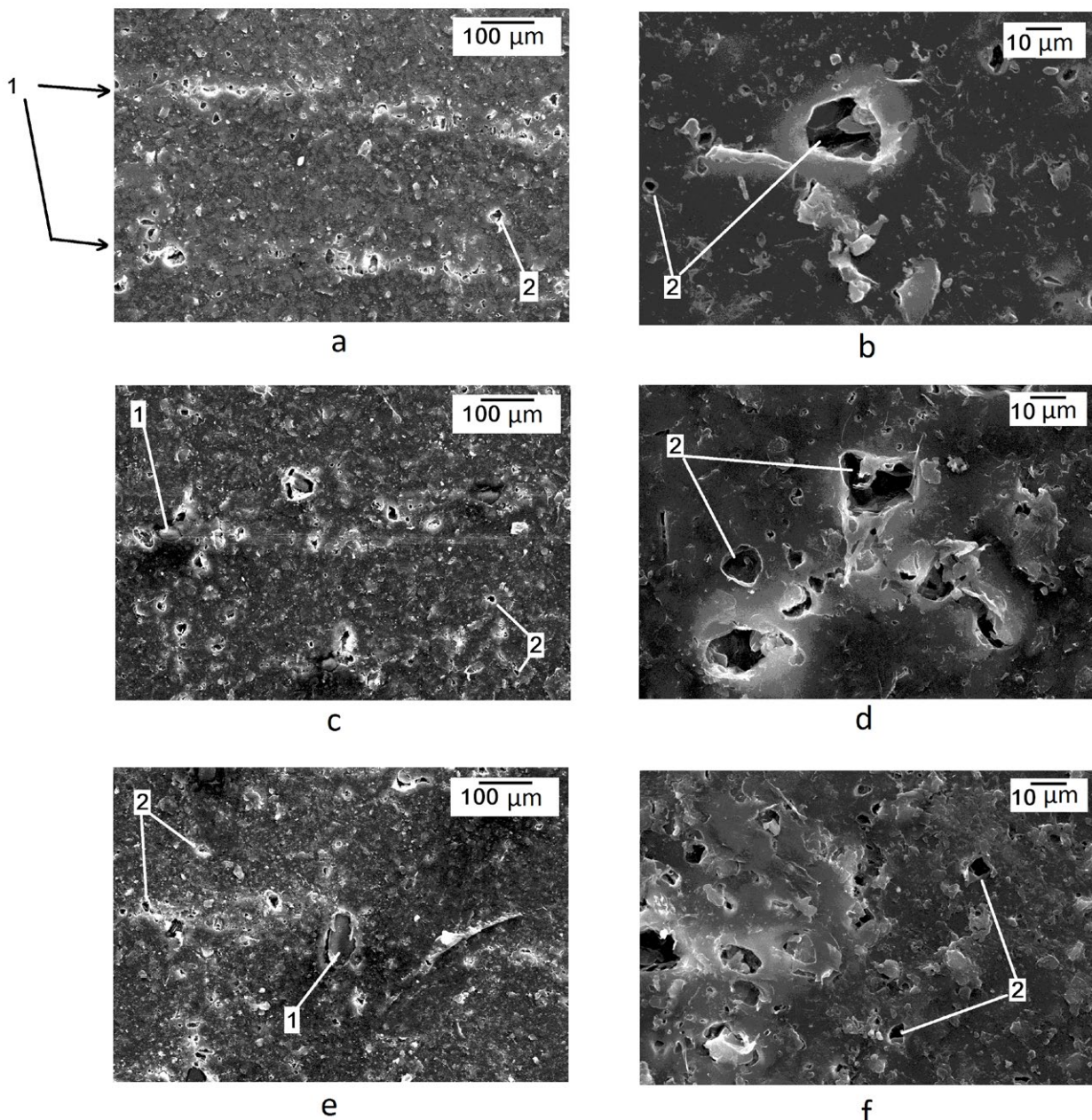


Fig. 5. SEM images of the surface of the anion exchange membranes under study: a, b – AEM_{prist}; c, d – AEM₁; e, f – AEM₂; a, c, e – magnification $\times 150$; b, d, f – magnification $\times 1000$

anion-exchange membranes, and fragments of reinforcing tissue are also visible for AEM₁ and AEM₂. For AEM_{prist} (Fig. 5a) the reinforcing fabric is not explicitly detected on the surface, however, there is a noticeable violation of the uniformity of distribution of the polyethylene/ion exchanger composite over the threads of the reinforcing fabric. As the time of using AEM in the electrodialyzer increases, the reinforcing fabric reaches the surface (Fig. 5, c, e): polyester

fragments up to 60×40 microns in size for AEM₁, enlarging to 160×60 microns for AEM₂, are visualized on the SEM images. An increase in the size of the sections of reinforcing fabric extending to the surface naturally leads to an increase in the gaps between the reinforcement strands and the polyethylene/ion exchanger composite material. To assess the changes in the state of the cavities and walls, the membrane sections located between the strands of the reinforcing

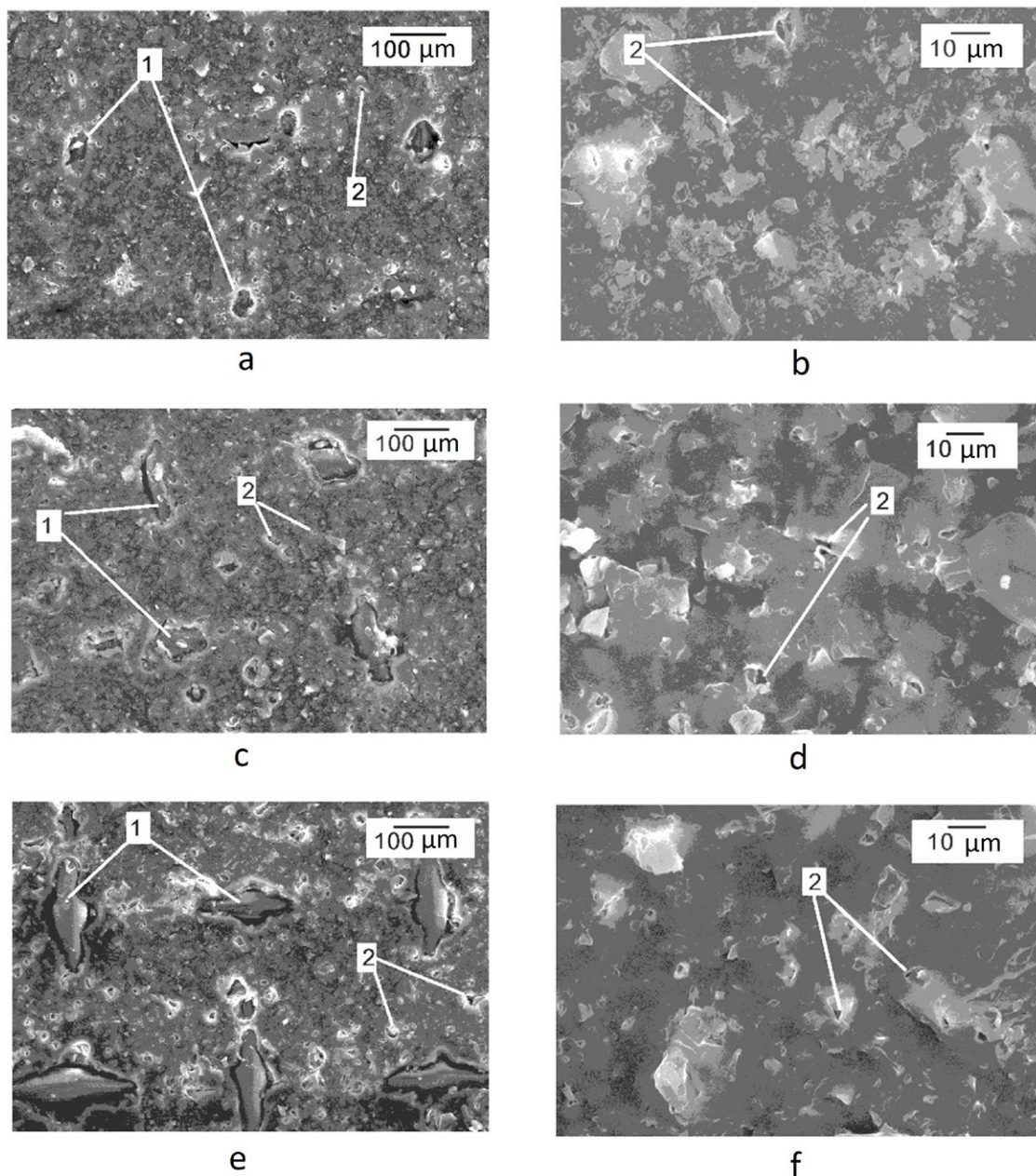


Fig. 6. SEM images of the surface of the cation exchange membranes under study: a, b – $\text{CEM}_{\text{prist}}$; c, d – CEM_1 ; e, f – CEM_2 ; a, c, e - magnification $\times 150$; b, d, f – magnification $\times 1000$

mesh were examined at a higher magnification (Fig. 5b, d, e). For $\text{AEM}_{\text{prist}}$, the size of the voids reaches 24 microns. As the operating time of the IEM increases, the size of the caverns does not increase, however, there is an increase in their number. In the case of cation exchange membranes (Fig. 6), a larger (compared to AEM) fraction of the surface is occupied by reinforcing tissue. The main change found during the operation of cation exchange membranes in the

electrodialyzer is the appearance of reinforcing fabric on the surface: the size of polyester filaments found on the SEM images of IEM increases in the $\text{CEM}_{\text{prist}} < \text{CEM}_1 < \text{CEM}_2$ range and amounts to (microns): 4×3, 13×6, and 15×6, respectively.

Thus, the analysis of the SEM images shows that, compared with the conditioned $\text{CEM}_{\text{prist}}$ and $\text{AEM}_{\text{prist}}$ samples, prolonged operation led to a more noticeable manifestation of defects caused

by the formation of cavities and the appearance of reinforcing tissue on the surface. Both cationic (CEM_1 , CEM_2) and anion-exchange (AEM_1 , AEM_2) membranes are characterized by an increase in the content of macropores formed between the reinforcing fabric and the ion exchanger + polyethylene composite.

In addition, the presence of large [50, 51] and highly hydrated [50, 52, 53] ions in the processed solutions can lead to stretching of the IEM matrix and, consequently, an increase in the size of the pores filled with solution or water. The latter is supported by the observed increase in the thickness of the initial and spent membranes, which swelled under the same conditions (Table 1). In turn, an increase in the content of strongly bound water may be due to an increase in the distance between fixed groups of the ion-exchange material during the degradation of the crosslinking agent, as was shown by the example of the KU-2 sulfocation ion exchanger with different divinylbenzene content [33].

4. Conclusion

The moisture content and thermal effect of dehydration of cation exchange (RalexCMH-Pes) and anion exchange (RalexAMH-Pes) membranes were thermogravimetrically determined before and after their long-term use in industrial electrodialysis plants during the concentration/desalination of multicomponent salt solutions, waste products from the production of complex mineral fertilizers. It was found that the moisture capacity of the membranes and the specific heat of dehydration, regardless of the type of membrane, increase with increasing duration of operation of the electrodialyzer. The molar thermal effect is practically independent of the type of membrane and the duration of its use and averages 39.0 ± 1.8 and 35.8 ± 1.2 kJ/mol for cation-exchange and anion-exchange membranes, respectively, which corresponds to the formation of associates of 2–4 water molecules.

The estimation of the total and relative content of kinetically unequal water molecules in the membranes showed the highest fraction of weakly and moderately bound water, which ranges from 87.0 to 90.2 % for cation exchange membranes and 79.3 to 85.0 % for anion exchange membranes. The contribution of water molecules

involved in the strong ion-dipole interaction with the functional groups of the membrane is the smallest. The nature of changes in the content of water molecules with different degree of binding depends on the type of membrane depending on the time of use: if for cation exchange membranes during operation the proportion of strongly bound water increases from 9.6 to 13.0 %, then in the case of anion exchange membranes, on the contrary, it decreases from 19.3 to 15.0 %.

The discovered effects of an increase in moisture content and a redistribution of water fractions of different degree of binding can be explained by an increase in the number of defects (cavities) and the release of reinforcing tissue onto the membrane surface, as well as an increase in the size of macropores filled with solution or water. These changes in membrane morphology may be caused by membrane degradation during prolonged operation in an electrodialysis unit. A feature of anion exchange membranes is the diffractometrically confirmed formation of inorganic precipitation, the hydrophilic particles of which are localized in the nanopores of the membrane, which probably contributes to an additional increase in the moisture content of the anion exchange material.

Contribution of the authors

Kozaderova O. A. – head of the grant, idea, scientific guidance, research concept, development of methodology, conducting research, writing a paper. Saranov I. A. – conducting research.

Conflict of interests

The authors declare that they have no known competing financial interests or personal relationships that could have influenced the work reported in this paper.

References

1. Al-Amshawee S., Yunus M. Y. B. M., Azoddein A. A. M., Hassell D. G., Dakhil I. H., Hasan H. A. Electrodialysis desalination for water and wastewater: a review. *Chemical Engineering Journal*. 2020;380: 122231. <https://doi.org/10.1016/j.cej.2019.122231>
2. Fadillah G., Hidayat R., Saputra A., ... Ohira S.-I. Advanced electrodialysis techniques for analytical separation: a comprehensive review. *Analytica Chimica Acta*. 2025; 344637. <https://doi.org/10.1016/j.aca.2025.344637>
3. Konarev A. Use of electrodialysis in the pilot- and commercial-scale production of pharmaceutical substances.

Russian Journal of Electrochemistry. 2015;51: 1124–1134. <https://doi.org/10.1134/S1023193515110051>

4. Wang M., Kuang S., Wang X., ... Zhang Y. Transport of amino acids in soy sauce desalination process by electrodialysis. *Membranes.* 2021;11: 408. <https://doi.org/10.3390/membranes11060408>

5. Mohammadi R., Tang W., Sillanpää M. A systematic review and statistical analysis of nutrient recovery from municipal wastewater by electrodialysis. *Desalination.* 2021;498: 114626. <https://doi.org/10.1016/j.desal.2020.114626>

6. Xie M., Shon H. K., Gray S. R., Elimelech M. Membrane-based processes for wastewater nutrient recovery: technology, challenges, and future direction. *Water Research.* 2015;89: <https://doi.org/10.1016/j.watres.2015.11.045>

7. Ferrari F., Pijuan M., Molenaar S., ... Radjenovic J. Ammonia recovery from anaerobic digester centrate using onsite pilot scale bipolar membrane electrodialysis coupled to membrane stripping. *Water Research.* 2022;218: 118504. <https://doi.org/10.1016/j.watres.2022.118504>

8. Vineyard D., Hicks A., Karthikeyan K., Davidson Ch., Barak Ph. Life cycle assessment of electrodialysis for sidestream nitrogen recovery in municipal wastewater treatment. *Cleaner Environmental Systems.* 2021;2: 100026. <https://doi.org/10.1016/j.cesys.2021.100026>

9. Mondor M., Masse L., Lamarche F., Massé D. Use of electrodialysis and reverse osmosis for the recovery and concentration of ammonia from swine manure. *Bioresource technology.* 2008;99: 7363–8. <https://doi.org/10.1016/j.biortech.2006.12.039>

10. Pismenskaya N. D., Rybalkina O. A., Tsygurina K. A., ... Bazinet L. Production of cheap phosphorus-ammonium fertilizers using electrodialysis. Problems and solutions. In: *Membrane process modeling: abstracts of the international conference dedicated to the 60th anniversary of Professor A. N. Filippov. December 3–4, 2020, Moscow.* Moscow: Logos Publ.; 2020. P. 68–69. Available at: https://kvm.gubkin.ru/Abstracts_RGU.pdf

11. Huang Ch., Xu T., Zhang Y., Xue Y., Chen G. Application of electrodialysis to the production of organic acids: State-of-the-art and recent developments. *Journal of Membrane Science.* 2007;288: 1. <https://doi.org/10.1016/j.memsci.2006.11.026>

12. Bagastyo A. Y., Anggrainy A. D., Nindita C. S., Warmadewanthi. Electrodialytic removal of fluoride and calcium ions to recover phosphate from fertilizer industry wastewater. *Sustainable Environment Research.* 2017;27(5): 230–237. <https://doi.org/10.1016/j.serj.2017.06.002>

13. Hikmawati D., Bagastyo A., Warmadewanthi I. Electrodialytic recovery of ammonium and phosphate ions in fertilizer industry wastewater by using a continuous-flow reactor. *Journal of Ecological Engineering.* 2019;20: 255. <https://doi.org/10.12911/22998993/109461>

14. Niftaliev S. I., Kozaderova O. A., Kim K. B., Malyavina Yu. M., Electrodialysis in the treatment of nitrogen-containing wastewater of a mineral fertilizer manufacturing enterprise*. *Chemical Industry Developments.* 2014;7: 52. (in Russ.). Available at: <https://elibrary.ru/item.asp?id=22017822>

15. Bokhary A., Tikka A., Leitch M., Liao B.Q. Membrane fouling prevention and control strategies in pulp and paper industry applications: a review. *Membrane.* 2018;4(4): 181. <https://doi.org/10.22079/jmsr.2018.83337.1185>

16. Apel P. Yu., Velizarov S., Volkov A. V., Yaroslavtsev A. B. Fouling and membrane degradation in electromembrane and baromembrane processes. *Membranes and Membrane Technologies.* 2022;4: 69–92. <https://doi.org/10.1134/S2517751622020032>

17. Gally C. R., Benvenuti T., Trindade C. M., ... Bernardes A. M. Electrodialysis for the tertiary treatment of municipal wastewater: Efficiency of ion removal and ageing of ion exchange membranes. *Journal of Environmental Chemical Engineering.* 2018;6(5): 5855–5869. <https://doi.org/10.1016/j.jece.2018.07.052>

18. Vasil'eva V. I., Akberova E. M., Kostylev D. V., Tzkhai A. A. Diagnostics of the structural and transport properties of an anion-exchange membrane MA-40 after use in electrodialysis of mineralized natural waters. *Membranes and Membrane Technologies.* 2019;1(3): 153–167. <https://doi.org/10.1134/S2517751619030077>

19. Vasil'eva V. I., Akberova E. M., Goleva E. A., Yatsev A. M., Tzkhai A. A. Changes in the microstructure and operational characteristics of the MK-40 sulfocation-exchange membrane during the electrodialysis of natural waters. *Journal of Surface Investigation: X-Ray, Synchrotron and Neutron Techniques.* 2017;11(2): 429–436. <https://doi.org/10.1134/S1027451017020367>

20. Pasechnaya E. L., Ponomar M. A., Klevtsova A. V., Korshunova A. V., Sarapulova V. V., Pismenskaya N. D. Characteristics of aliphatic and aromatic ion-exchange membranes after electrodialysis tartrate stabilization of wine materials. *Membranes and Membrane Technologies.* 2024;14(4): 317–332. <https://doi.org/10.31857/S2218117224040079>

21. Ghalloussi R., Garcia-Vasquez W., Bellakhal N., ... Grande D. Ageing of ion-exchange membranes used in electrodialysis: Investigation of static parameters, electrolyte permeability and tensile strength. *Separation and Purification Technology.* 2011;80(2): 270–275. <https://doi.org/10.1016/j.seppur.2011.05.005>

22. Ghalloussi R., Chaabane L., Dammak L., Grande D. Ageing of ion-exchange membranes used in an electrodialysis for food industry: SEM, EDX, and limiting current investigations. *Desalination and Water Treatment.* 2015;56(10): 2561–2566. <https://doi.org/10.1080/19443994.2014.968908>

23. Kharina A. Yu., Charushina O. E., Eliseeva T. V. Organic fouling of anion-exchange and bipolar membranes during the separation of amino acid and sucrose by electrodialysis. *Condensed Matter and Interphases..* 2023;25(2): 268–276. <https://doi.org/10.17308/kcmf.2023.25/11107>

24. Vasil'eva V. I., Akberova E. M., Shaposhnik V. A., Malykhin M. D. Electrochemical properties and structure of ion-exchange membranes upon thermochemical treatment. *Russian Journal of Electrochemistry.* 2014;50(8): 789–797. <https://doi.org/10.1134/S102319351408014X>

25. Vasil'eva V. I., Akberova E. M., Pismenskaya N. D., Nebavskaya K. A. Effect of thermochemical treatment on the surface morphology and hydrophobicity of heterogeneous ion-exchange membranes. *Russian Journal of Physical Chemistry A.* 2014;88(8): 1293–1299. <https://doi.org/10.1134/S0036024414080317>

26. Volodin D. N., Magomedova N. V., Voropayev A. N. The use of electromembrane technology in wastewater treatment. *Vodoochistka. Vodopodgotovka. Vodosnabzhenie.*

2015;92(8): 32–36. (In Russ.). Available at: <https://elibrary.ru/item.asp?id=24146800>

27. Kozaderova O. A., Kim K. B., Niftaliyev S. I. Changes of physicochemical and transport characteristics of ion exchange membranes in the process of operation under demineralization of wastewater water production of nitrogen-containing mineral fertilizers *Sorbtionnye I Khromatograficheskie Protessy*. 2018;18(6): 875–885. (in Russ.). <https://doi.org/10.17308/sorpchrom.2018.18/616>

28. Han L. Aging and degradation of ion-exchange membranes. In: *Zhang Z., Zhang W., Chehimi M.M. (eds.) Membrane technology enhancement for environmental protection and sustainable industrial growth. Advances in Science, Technology & Innovation*. 2021. Springer, Cham. https://doi.org/10.1007/978-3-030-41295-1_3

29. Shaposhnik V. A. The role of hydration in ion exchange separations. Kinetics and dynamics of metabolic processes*. In: *Fundamental problems of Separation Science: Abstracts of the VIII All-Russian Symposium with international participation, November 18–22, 2019, Moscow*. Moscow: Publishing House “Frontier”; 2019. p. 34–36. (in Russ.). Available at: <https://elibrary.ru/item.asp?id=44353630&selid=44353758>

30. Safranova E. Y., Yaroslavtsev A. B., Volkov V. I., Pavlov A. A., Chernyak A. V., Volkov E. V. Hydration of the H⁺, Li⁺, Na⁺, and Cs⁺ ions in MF-4SK perfluorinated sulfonic acid cation-exchange membranes modified with inorganic dopants. *Russian Journal of Inorganic Chemistry*. 2011;56(2): 156–162. <https://doi.org/10.1134/S0036023611020240>

31. Zyryanova S., Mareev S., Gil V., ... Dammak L. How electrical heterogeneity parameters of ion-exchange membrane surface affect the mass transfer and water splitting rate in electrodialysis. *International Journal of Molecular Sciences*. 2020;21(3): 973. <https://doi.org/10.3390/ijms21030973>

32. Kharina A. Yu., Eliseeva T. V. Cation-exchange membrane MK-40 characteristics in electrodialysis of mixed solutions of mineral salt and amino acid. *Sorbtionnye I Khromatograficheskie Protessy*. 2017;17(1): 148–155. (in Russ.). <https://doi.org/10.17308/sorpchrom.2017.17/364>

33. Kotova D. L., Selemenev V. F. *Thermal analysis of ion-exchange materials**. Moscow: Nauka Publ.; 2002. 157 p. (in Russ.)

34. Kononenko N., Nikonenko V., Grande D., ... Volkovich Yu. Porous structure of ion exchange membranes investigated by various techniques *Advances in Colloid and Interface Science*. 2017;246: 196–216. <https://doi.org/10.1016/j.cis.2017.05.007>

35. Sarapulova V. V., Titorova V. D., Nikonenko V. V., Pismenskaya N. D. Transport characteristics of homogeneous and heterogeneous ion-exchange membranes in sodium chloride, calcium chloride, and sodium sulfate solutions. *Membranes and Membrane Technologies*. 2019;1(3): 168–182. <https://doi.org/10.1134/S2517751619030041>

36. Krisilova E. V., Eliseeva T. V., Oros G. Y. Effect of amino acid sorption on formation of water clusters in ion-exchange membranes. *Colloid Journal*. 2011;73(1): 72–75. <https://doi.org/10.1134/S1061933X11010091>

37. <https://www mega.cz/membranes/#what-we-do>

38. Niftaliyev S. I., Kouznetsova I. V., Peregoudov Yu. S., Okshin V. V., Melnik A. V. Prospects for utilization of sewage from the “FERTILIZERS” open joint-stock company. *Ecology*

and *Industry of Russia*. 2012;(5): 36–39. (In Russ.). <https://doi.org/10.18412/1816-0395-2012-5-36-39>

39. Kononenko N. A., Demina O. A., Loza N. V., Falina I. V., Shkirskaya S. A. *Membrane electrochemistry**. Krasnodar: Kubanskii gosudarstvennyi universitet Publ.; 2015. 290 p. (In Russ.)

40. Kozaderova O. A. Electrochemical characterization of an MB-2 bipolar membrane modified by nanosized chromium(III) hydroxide. *Nanotechnologies in Russia*. 2018;13(9–10): 508–515. <https://doi.org/10.1134/S1995078018050075>

41. Astapov A. V., Peregudov Y. S., Kopylova V. D. The state of water in different forms of sulfo ion-exchange fiber. *Russian Journal of Physical Chemistry A*. 2011;85(7): 1253–1256. <https://doi.org/10.1134/S0036024411070028>

42. Yaroshenko F. A. *Proton conductivity of composite materials based on polymers modified with polysulfuric acid**. Cand. chem. sci. diss. Chelyabinsk: 2020. 131 p. Available at: <https://www.dissertcat.com/content/protonnaya-provodimost-kompozitsionnykh-materialov-na-osnove-polimerov-modifitsirovannykh/read>

43. Vainertova K., Krshivchik I., Nedela D., ... Movsumzade E. M. Polymer binders for ion-exchange membranes with improved mechanical strength. *Industrial Production and Use Elastomers*. 2016;2: 33–42. (In Russ.). Available at: <https://www.elibrary.ru/item.asp?id=26599727>

44. Eliseeva T. V., Zyablov A. N., Kotova D. L., Selemenev V. F. Hydration of ion-exchange membranes saturated with amino acids. *Russian Journal of Physical Chemistry A*. 1999;73(5): 783–785. Available at: <https://www.elibrary.ru/item.asp?id=13321063>

45. Zyablov A. N. Hydration of amino acids and ion-exchange membranes in amino acid forms and its effect on diffusion transport*. Cand. chem. sci. diss. Voronezh: 1999. 162 p. Available at: <https://www.dissertcat.com/content/gidratisiya-aminokislot-i-ionoobmennykh-membran-v-aminokislotnykh-formakh-i-ee-vliyanie-na>

46. Zyablov A. N., Eliseeva T. V., Kotova D. L. Thermal analysis as a method for studying the hydration of ion-exchange membranes in amino acid forms*. *Teoriya i praktika sorbtionnykh protessov*. 1999;24: 57–58. (In Russ.)

47. Kozaderova O. A., Sinyaeva L. A., Khukharkina Y. S. Contact-difference method for measuring electrical conductivity in determination of the transport characteristics of heterogeneous ion-exchange membranes of different service life in an industrial electrodialyzer. *Sorbtionnye I Khromatograficheskie Protessy*. 2025;25(3): 316–327. (in Russ.). <https://doi.org/10.17308/sorpchrom.2025.25/13043>

48. Porozhny M. V. Electrochemical characteristics of ion-exchange membranes with organic and inorganic immobilized nanoparticles*. Cand. chem. sci. diss. Krasnodar: 2018. 112 p. (in Russ.)

49. Yurova P. A., Karavanova Y. A., Stenina I. A., Yaroslavtsev A. B. Synthesis and studies on the diffusion properties of MK-40 cation-exchange membranes modified with ceria. *Nanotechnologies in Russia*. 2016;11(11–12): 761–765. <https://doi.org/10.1134/S1995078016060215>

50. Helfferich F. G. *Ionenaustauscher. Band 1: Grundlagen. Struktur - Herstellung – Theorie*. Weinheim: Verlag Chemie; 1959.

51. Pismenskaya N., Sarapulova V., Nevakshenova E., Kononenko N., Fomenko M., Nikonenko V. Concentration

dependencies of diffusion permeability of anion-exchange membranes in sodium hydrogen carbonate, monosodium phosphate, and potassium hydrogen tartrate solutions. *Membranes*. 2019;9: 170. <https://doi.org/10.3390/membranes9120170>

52. Kononenko N. A., Berezina N. P. Research methods and characterization of synthetic polymer membranes. In: *Membranes and Membrane technologies**. Moscow: Nauchny Mir Publ., 2013. p. 402–455. (in Russ.)

53. Koga Y., Kondo T., Miyazaki Y., Inaba A. The effects of sulphate and tartrate ions on the molecular organization of water: towards understanding the hofmeister series (VI). *Journal of Solution Chemistry*. 2012;41: 1388–1400. <https://doi.org/10.1007/s10953-012-9880-x>

* Translated by author of the article

Information about the authors

Olga A. Kozaderova, Professor, Dr. Sci. (Chem.), Professor at the Department of Inorganic Chemistry and Chemical Technology, Voronezh State University of Engineering Technologies (Voronezh, Russian Federation).

<https://orcid.org/0000-0002-8135-5801>
kozaderova-olga@mail.ru

Igor A. Saranov, Cand. Sci. (Tech.), Associate Professor at the Department of Information Security, Voronezh State University of Engineering Technologies (Voronezh, Russian Federation).

<https://orcid.org/0000-0002-9510-5168>
mr.saranov@mail.ru

Received August 11, 2025; accepted after reviewing November 13, 2025; accepted for publication November 17, 2025; published online December 25, 2025.